

## Electron Conductive Three-Dimensional Polymer of Cuboidal C<sub>60</sub>

Shoji Yamanaka,<sup>1</sup> Akira Kubo,<sup>1</sup> Kei Inumaru,<sup>1</sup> Kenji Komaguchi,<sup>1</sup> N. S. Kini,<sup>1</sup> Toru Inoue,<sup>2</sup> and Tetsuo Irifune<sup>2</sup>

<sup>1</sup>Department of Applied Chemistry, Graduate School of Engineering, Hiroshima University, Higashi-Hiroshima 739-8527, Japan

<sup>2</sup>Ultra-high Pressure Laboratory, Geodynamics Research Center, Ehime University, Bunkyo-cho 2-5, Matsuyama 790-8577, Japan

(Received 6 May 2005; published 22 February 2006)

Single crystals of three-dimensional (3D) C<sub>60</sub> polymer were prepared by the topotactic conversion of two-dimensional (2D) C<sub>60</sub> polymer single crystals at a pressure of 15 GPa at 600 °C. The x-ray single crystal study revealed that the 3D C<sub>60</sub> polymer crystallized in a body centered orthorhombic space group *Immm*, and spherical C<sub>60</sub> monomer units were substantially deformed to rectangular parallelepiped (cuboidal) shapes, each unit being bonded to eight cuboidal C<sub>60</sub> neighbors via [3 + 3] cycloaddition. The 3D C<sub>60</sub> polymer was electron conductive, in contrast with the nonconductive behavior of 2D polymers.

DOI: 10.1103/PhysRevLett.96.076602

PACS numbers: 72.80.Le, 81.05.Tp, 81.05.Uw, 81.07.-b

C<sub>60</sub> molecules, consisting of a large number of C=C double bonds, are easily polymerized via [2 + 2] cycloaddition of the hexagon-hexagon double bonds on adjacent molecules [1]. Orthorhombic one-dimensional (1D) and two types of two-dimensional (2D) C<sub>60</sub> polymers are formed under high pressure and high temperature (HPHT) conditions [2,3]: orthorhombic 2D (O-2D) polymer is formed at pressures below 3 GPa at 500 °C, while rhombohedral 2D (R-2D) polymer is obtained at higher pressures. In these 2D polymers, each C<sub>60</sub> unit is bonded two-dimensionally to four and six first neighbors, respectively, via [2 + 2] cycloaddition within the plane. The 2D polymers are relatively soft due to the weak van der Waals interaction between the planes and exhibit no electron conduction [4]. Under much higher pressures ( $P > 13$  GPa) at elevated temperatures, three-dimensional (3D) polymers are obtained, in which C<sub>60</sub> molecules are covalently bonded to form a strong 3D network [5–9]. Some of the 3D C<sub>60</sub> polymers are reported to be extremely hard and have bulk moduli even larger than those of diamonds [10,11].

Structural models of 3D C<sub>60</sub> polymers have been proposed [5,6,8], where the C<sub>60</sub> molecules are suggested to be three-dimensionally polymerized to form zeolitelike or clathratelike carbon networks. However, due to the poor powder x-ray diffraction data available, reliable crystal structures and the nature of bonding between the C<sub>60</sub> molecules have remained unclear. In this study, we have succeeded in synthesizing single crystals of 3D C<sub>60</sub> polymers under HPHT conditions for the first time, which allow us to perform their structural analyses.

The two types of single crystals of 2D C<sub>60</sub> polymers were first prepared from C<sub>60</sub> monomer single crystals as described elsewhere [12,13]. The 2D polymer single crystals were then embedded in hexagonal BN (h-BN) powder and filled in a cylindrical h-BN cell, which was surrounded by a thin Pt-tube heater. The whole sample assembly was compressed in a Kawai-type multianvil apparatus [14] up to 15 GPa, followed by heating to temperatures in a range of 500–700 °C in 5 min. After keeping the sample at the temperature for 1 h, it was cooled down to room tempera-

ture in 30 min. Then the pressure was gradually released over matrix. The single crystal structural analysis was carried out by an x-ray diffractometer with an imaging plate (IP) detector (Rigaku-RAXIS) using graphite monochromated Mo  $K\alpha$  radiation ( $\lambda = 0.71073$  Å). Geometry optimization of the 3D C<sub>60</sub> polymer was performed using the DMOL3 Solid State program [15–17] with double numerical atomic basis sets (DND), and the Perdew-Wang local-density approximation functional. The convergence tolerance quality level of self-consistent field was medium with settings  $2.0 \times 10^{-5}$  Ha (1 Ha = 27.2 eV) of the energy, 0.004 Ha/Å for the maximum force, and 0.005 Å for the maximum displacement.

Single crystals of two types of 2D C<sub>60</sub> polymers, O-2D [ $a = 9.026(2)$ ,  $b = 9.083(2)$ ,  $c = 15.077(3)$  Å] and R-2D [ $a = 9.175(1)$ ,  $c = 24.568(3)$  Å] [12,13] were irreversibly converted into new structures at 15 GPa at 600 °C; O-3D [ $a = 7.86(2)$ ,  $b = 8.59(2)$ ,  $c = 12.73(4)$  Å], and R-3D [ $a = 9.19(1)$ ,  $c = 21.99(7)$  Å] polymers, respectively. Note that the 2D to 3D conversion under high pressure occurs topochemically, keeping the basic structure of the individual 2D polymers. Detailed single crystal analysis of the R-3D polymer is currently under way, and here we focus the structure of the O-3D polymer (hereafter, 3D polymer).

One single crystal ( $0.3 \times 0.2 \times 0.2$  mm<sup>3</sup>) of the 3D polymer was found and selected for x-ray structural study from more than 70 grains examined. The sample contained a considerable amount of the 2D polymer, and the IP oscillation photograph taken around the  $a^*$  axis had the reflection 200 of the 3D polymer associated with the reflection 200 of the O-2D polymer on the rotation axis [18]. This observation confirms that the O-2D polymer crystal shrunk topochemically to form the 3D polymer, as suggested in the above paragraph. The reflection data of 1089 peaks were collected in a range  $2\theta < 34^\circ$ . The numbers of unique reflections used were 161 for all data and 107 for  $I > 2\sigma(I)$  after merging [18]. The small number of observed reflections, the presence of a substantial amount of a different phase, and the relatively poor con-

sistency of symmetry-equivalent reflections ( $R_{\text{int}} = 7.74\%$ ) imply that the refined geometry is qualitatively correct, but that bond lengths and angles have larger error limits than what are usual from crystallographic measurements. The systematic absences of reflections supported that the cell was body centered, and the space group should be attributed to *Immm*, the same space group as that of the starting O-2D polymer phase. An attempt to solve the structure by direct methods failed due to the small number of unique reflections available against the number of parameters to be determined. Then, the starting coordinates of 9 crystallographically independent carbon sites ( $6 \times 16o$ ,  $8m$ ,  $8n$ , and  $8l$ ) were taken from the O-2D polymer structure [13], and the positions were modified using loose restraints (DFIX) of the C-C bond lengths in a range of 1.3–1.7 Å by SHELX97 software [19]. The final refinements were performed using full matrix least squares after removing all of the restraints. The  $R1$  values converged to 11.89% and 13.90% for  $I > 2\sigma(I)$  and all data, respectively, for 74 variables including anisotropic parameters. The residual electron densities,  $\Delta\rho_{\text{max}}$  and  $\Delta\rho_{\text{min}}$ , were +0.309 and  $-0.319e/\text{Å}^3$ , respectively. The atomic coordinates are given in Table I. The measured density ( $2.55 \text{ g/cm}^3$ ) of the 3D polymer by an Archimedes method using a heavy aqueous solution of sodium polytungstate is slightly smaller than that calculated from the lattice parameters ( $2.78 \text{ g/cm}^3$ ), presumably due to the remnant of the starting 2D polymer. The amount of the low-density 2D polymer present in the 3D crystal is estimated to be about 30%. In fact, the optimum temperature for the formation of the 3D polymer was so limited that it was difficult to obtain pure 3D polymer crystals in the present study: a graphite-like amorphous phase was observed in the 3D polymer at temperatures higher than  $700^\circ\text{C}$ , whereas only a small part of the 2D polymer was converted to the 3D polymer at temperatures below  $550^\circ\text{C}$ .

The structure of the 3D polymer derived from the present x-ray diffraction data is compared with that of the starting 2D polymer in Fig. 1. Note that the individual  $\text{C}_{60}$  unit in the 3D polymer is much deformed into a

rectangular parallelepiped (cuboid). Each cuboid is linked to 8 cuboid neighbors in the body centered cell by  $[3 + 3]$  cycloaddition, forming  $\text{C1-C5}^*$  and  $\text{C5-C1}^*$  intermolecular bonds (1.41 Å) at the eight corners.

In the 2D polymer, the  $\text{C}_{60}$  units are linked to each other by the  $[2 + 2]$  cycloaddition, the centers of the  $\text{C}_{60}$  units being separated at a distance of 9.0 Å. In the 3D polymer, the distances between the centers of the cuboids are substantially reduced to 7.86(2) and 8.59(2) Å along the  $a$  and  $b$  axes, respectively. Note that the  $\text{C7-C7}^*$  intermolecular bonds (bond length = 1.6 Å) found in the 2D polymer layers are broken and enlarged to 2.47 Å in the 3D polymer to form intramolecular  $\text{C7=C7}$  double bonds, which are slightly pushed back into the cuboid due to the strong repulsion between the facing  $\pi$  bonds as shown in Figs. 1(b) and 1(c).

The refined data show that all of the carbon sites have similar large atomic displacement factors ( $U_{\text{eq}}$ ) of about 0.2, which are much larger than the values of the 2D polymer of about 0.04 [12,13]. This is probably caused by a combination of fluctuation of the structure and poor crystallinity of the 3D polymer. To check the stability of the arrangement of the carbon atoms obtained in the present study, a geometry optimization was performed using DMOL3 Solid State software [15–17]. In order to check the reliability of the software in the present system, this method was first applied to the geometry optimization of the structure of the O-2D polymer using the accurate single crystal analysis data reported previously [13]. The calculation converged to an optimized structure with a total energy lower than that of the starting structure only by 33.7 kJ/mol of  $\text{C}_{60}$ , and all of the bond lengths were reproduced within an error of 0.02 Å. The accuracy of the density-functional theory method was also confirmed in the application to the R-2D  $\text{C}_{60}$  polymer [4].

The atomic coordinates obtained by the geometry optimization on the 3D polymer are compared with those determined by the x-ray refinement in Table I. The two data sets agree very well with each other, although some are slightly different. The largest disagreement is found in

TABLE I. Atomic coordinates for 3D  $\text{C}_{60}$  polymer refined in the *Immm* (No. 71) group with  $a = 7.86(2)$ ,  $b = 8.59(3)$ ,  $c = 12.73(4)$  Å, and  $Z = 2$ , in comparison with those by geometry optimization.

Atom	Site	X-ray refinement				Geometry optimization		
		$x$	$y$	$z$	$U_{\text{eq}}^a$	$x$	$y$	$z$
C1	16o	0.100(3)	0.341(3)	0.193(2)	0.16(1)	0.1015	0.3348	0.1920
C2	16o	0.180(3)	0.383(3)	0.097(2)	0.21(1)	0.1870	0.4019	0.0933
C3	16o	0.315(3)	0.277(3)	0.058(1)	0.19(1)	0.3200	0.2843	0.0554
C4	16o	0.147(3)	0.163(2)	0.205(2)	0.18(1)	0.1432	0.1650	0.1999
C5	16o	0.186(3)	0.400(2)	0.282(2)	0.15(1)	0.1902	0.4083	0.2823
C6	16o	0.361(3)	0.144(3)	0.116(2)	0.19(1)	0.3379	0.1403	0.1079
C7	8m	0.343(3)	0	0.051(2)	0.16(1)	0.3361	0	0.0518
C8	8l	0	0.078(4)	0.205(2)	0.17(2)	0	0.0800	0.1950
C9	8n	0.101(5)	0.613(5)	0	0.28(3)	0.0831	0.6298	0

<sup>a</sup> $U_{\text{eq}}$  ( $\text{Å}^2$ ), equivalent isotropic displacement parameters.

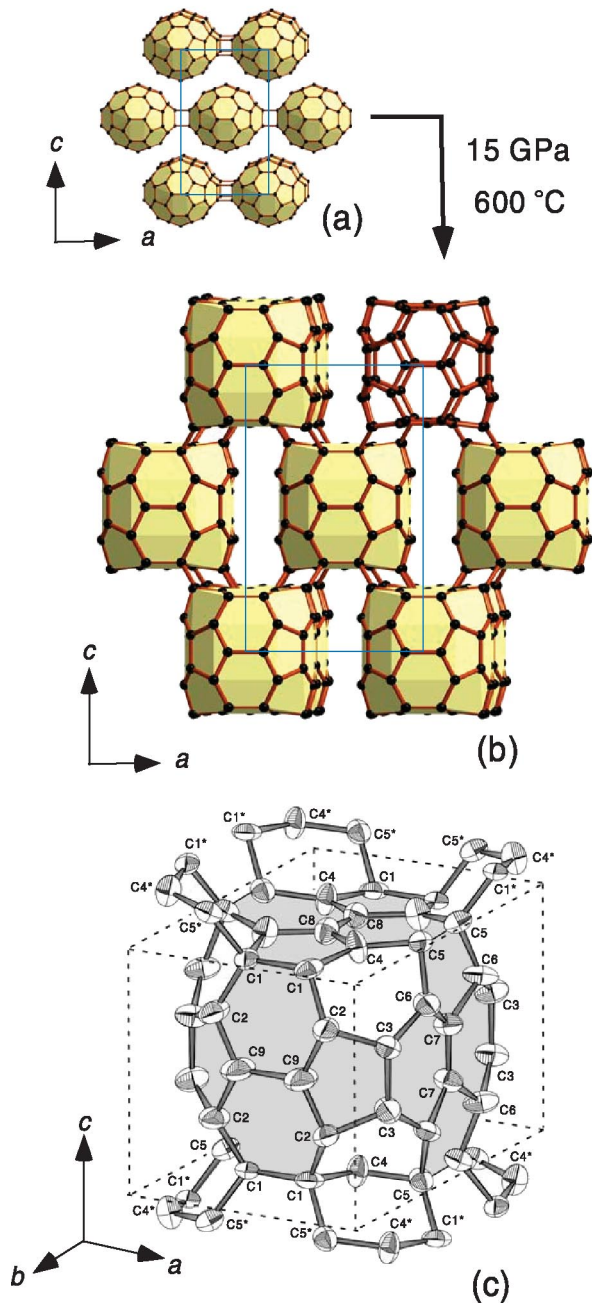


FIG. 1 (color). Crystal structure of the 3D C<sub>60</sub> polymer (b) in comparison with the starting 2D C<sub>60</sub> polymer (a). Carbon atoms marked with \* in (c) are from the neighboring C<sub>60</sub> units.

the atomic position of C9. The optimized intramolecular bond length C9=C9 is 1.306 Å, whereas it is 1.58 Å in the x-ray refinement. In the optimized structure, C9 atoms may form C9=C9 double bonds, which are pushed back into the C<sub>60</sub> cuboid as discussed for the C7=C7 carbon atoms. The optimized bond lengths C2-C2\* (1.685 Å) are shorter than 2.02(6) Å determined by the x-ray refinement, suggesting the formation of intermolecular single bonds. One of the reasons of the disagreement between the x-ray refined and the geometry optimized data could be found in the possible disorder of the carbon atoms at C9 sites. The

thermal ellipsoid of this atom is highly anisotropic with an elongation to the C9\* atoms of the adjacent C<sub>60</sub> units.

The band structure and the density of states (DOS) of the 3D C<sub>60</sub> polymer were calculated using the DMOL3 Solid State software [15] based on the coordinates obtained by the x-ray structural analysis, and the results are shown in Fig. 2(a). The band near the Fermi level ( $E_F$ ) is mainly composed of  $p$  orbitals; the 3D polymer should be metallic without a band gap around the Fermi level. The DOS curves of the geometry optimized model of the 3D polymer were also calculated, the general profile of which was very similar to those shown in Fig. 2(a) for the x-ray refined structural model over a wide energy range. However, the band near the Fermi level appears to be structure sensitive as compared in Fig. 2(b). The large DOS near the Fermi level of the x-ray refined model is much reduced in the DOS distribution for the geometry optimized model, which has a narrow gap of about 0.2 eV near the Fermi level.

The electrical conductivity of the 3D polymer was measured on some crystals with dimensions of about  $0.2 \times 0.2 \times 0.2$  mm<sup>3</sup> by a conventional 4 probe method in a temperature range of 4–300 K. The 3D polymer is electron conductive with a conductivity of about  $10^{-1}$ – $10^{-2}$  S cm<sup>-1</sup> at room temperature. The Arrhenius plot of the electrical conductivity ( $\sigma$ ) versus temperature ( $T$ ) was not linear; a typical sample gave very low activation energies of 0.3 and 7.8 meV at 4 and 300 K, respectively. The conductivity rather exhibits a power relation

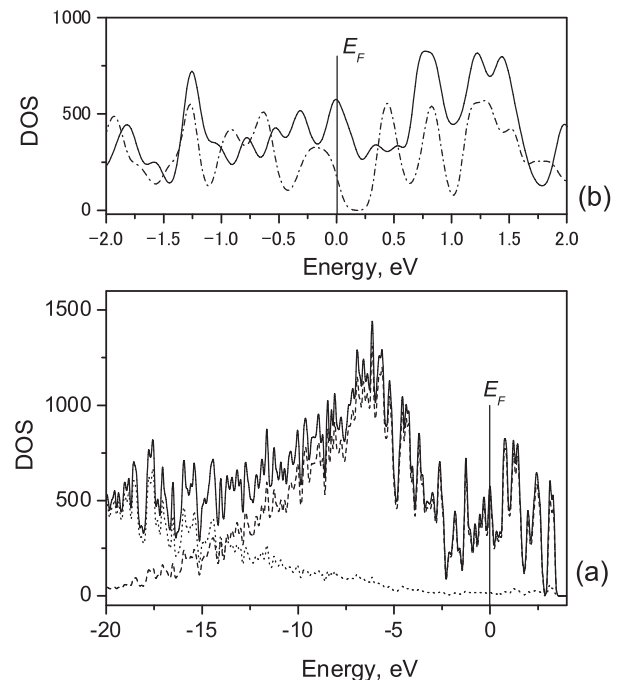


FIG. 2. Density of states of the 3D C<sub>60</sub> polymer; (a) the total DOS (solid line), and the partial DOS for  $s$  (dotted line) and  $p$  (dashed line) orbitals based on the x-ray refined structural model, and (b) the total DOS profiles near the Fermi level calculated on the structures determined by x-ray refinement (solid line) and geometry optimization (chained line).

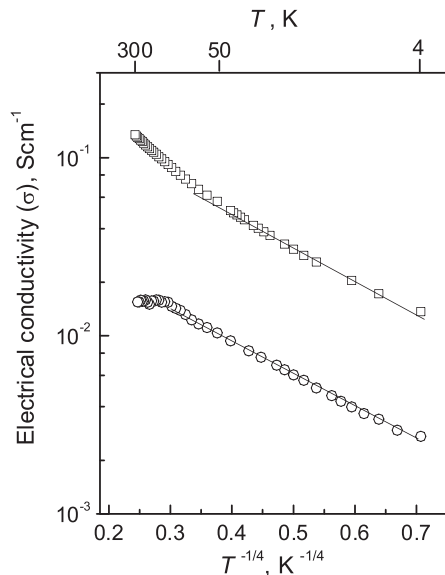


FIG. 3. Plot of  $\log \sigma$  versus  $T^{-1/4}$  for the 3D  $C_{60}$  polymer samples prepared at 600 °C (□) and 560 °C (○) at 15 GPa.

with temperature,  $\ln \sigma \propto T^{-1/4}$ , suggesting 3D Mott's variable range hopping (VRH). As shown in Fig. 3, the conductivity varied depending on the samples, even from the same preparation batch, but the slopes of the linear relation at the low temperature were very similar. It is well known that the conductivity of many conductive carbonaceous materials such as doped conjugated polymers and carbon nanotubes follows a 3D VRH hopping mechanism [20–22]. Recently, Buga *et al.* [23] reported that 3D  $C_{60}$  and  $C_{70}$  polymers prepared under a pressure of 11.5–13 GPa at temperatures 400–700 °C showed the 3D VRH, although the structures of the polymers were not known. The mechanism of VRH of these carbonaceous materials are interpreted in terms of lack of long-range order with localized states near the Fermi level. In our 3D polymer, although the DOS near the Fermi level suggests a metallic conductivity, similar lack of long-range order should be involved due to the nature of the samples such as low crystallinity, and the presence of disorder and dangling bonds.

The existence of three-dimensionally polymerized  $C_{60}$ , which would be formed via [2 + 2] cycloaddition under high pressure, was theoretically predicted [24]. The resulting  $sp^3$ - $sp^2$  hybridized system has been expected to show metallic conductivity. The 3D  $C_{60}$  polymer developed in this study has a different structure, containing [3 + 3] cycloaddition. The electrical properties of the conjugated system are structure sensitive, and we have not confirmed the metallic conductivity in the new 3D polymer. This is the first 3D crystalline carbon network containing  $sp^2$ - $sp^3$  carbon atoms. We hope that more detailed theoretical studies and spectroscopic measurements would be done in relation with the studies of carbon nanotubes and conjugated polymers.

This study has been supported by a Grant-in-Aid for Scientific Research (No. 16205027 and No. 170380320)

and the COE Research (No. 13E2002) of the Ministry of Education, Culture, Sports, Science, and Technology of Japan. The authors would like to thank Professor Craig Bina for his comments on the manuscript.

- [1] B. Sundqvist, in *Fullerenes*, edited by K.M. Kadish and R.S. Rudorff (Wiley, New York, 2000), Chap. 15.
- [2] Y. Iwasa *et al.*, *Science* **264**, 1570 (1994).
- [3] M. Núñez-Regueiro, L. Marques, J.-L. Hodeau, O. Bethoux, and M. Perroux, *Phys. Rev. Lett.* **74**, 278 (1995).
- [4] T. Miyake and S. Saito, *Chem. Phys. Lett.* **380**, 589 (2003).
- [5] V.D. Blank, S.G. Buga, G.A. Dubitsky, N.R. Serebryanaya, M. Yu. Popov, and B. Sundqvist, *Carbon* **36**, 319 (1998).
- [6] L.A. Chernozatonskii, N.R. Serebryanaya, and B.N. Mavrin, *Chem. Phys. Lett.* **316**, 199 (2000).
- [7] V.D. Blank, G.A. Dubitsky, N.R. Serebryanaya, B.N. Mavrin, V.N. Denisov, S.G. Buga, and L.A. Chernozatonskii, *Physica (Amsterdam)* **B339**, 39 (2003).
- [8] M. Mezouar, L. Marques, J.-L. Hodeau, V. Pischedda, and M. Núñez-Regueiro, *Phys. Rev. B* **68**, 193414 (2003).
- [9] E. Burgos, E. Halac, R. Weht, H. Bonadeo, E. Artacho, and P. Ordejon, *Phys. Rev. Lett.* **85**, 2328 (2000).
- [10] V. Blank, M. Popov, G. Pivovarov, K. Lvova, K. Gogolinsky, and V. Reshetov, *Diam. Relat. Mater.* **7**, 427 (1998).
- [11] V.D. Blank, S.G. Buga, N.R. Serebryanaya, V.N. Denisov, G.A. Dubitsky, A.N. Ivlev, B.N. Mavrin, and M. Yu. Popov, *Phys. Lett. A* **205**, 208 (1995).
- [12] X. Chen, S. Yamanaka, K. Sako, Y. Inoue, and M. Yasukawa, *Chem. Phys. Lett.* **356**, 291 (2002).
- [13] X. Chen and S. Yamanaka, *Chem. Phys. Lett.* **360**, 501 (2002).
- [14] N. Kawai and S. Endo, *Rev. Sci. Instrum.* **41**, 1178 (1970).
- [15] DMOL3 Solid State is available from Accelrys, San Diego, CA.
- [16] B. Delley, *J. Chem. Phys.* **92**, 508 (1990).
- [17] B. Delley, *J. Chem. Phys.* **113**, 7756 (2000).
- [18] See EPAPS Document No. E-PRLTAO-96-004609 for the IP oscillation photograph and the structure factor table. For more information on EPAPS, see <http://www.aip.org/pubservs/epaps.html>.
- [19] G.M. Sheldrick, computer code SHELX97, Program for Structure Refinement, University of Gottingen, Germany, 1997.
- [20] D. Schäfer-Siebert, C. Budrowski, H. Kuzmany, and S. Roth, in *Springer Series in Electronic Properties of Conjugated Polymers*, edited by H. Kuzmany, M. Mehring, and S. Roth (Springer, Berlin, 1987), p. 38.
- [21] J. Vavro, J.M. Kikkawa, and J.E. Fischer, *Phys. Rev. B* **71**, 155410 (2005).
- [22] R. Singh, A. Kaur, K.L. Yadav, and D. Bhattacharya, *Current Appl. Phys.* **3**, 235 (2003).
- [23] S.G. Buga, V.D. Blank, N.R. Serebryanaya, A. Dzwlowski, T. Makarova, and B. Sundqvist, *Diam. Relat. Mater.* **14**, 896 (2005).
- [24] S. Okada, S. Saito, and A. Oshiyama, *Phys. Rev. Lett.* **83**, 1986 (1999).